Crosslinker Chemistry Determines the Uptake Potential of Perfluorinated Alkyl Substances by β-Cyclodextrin Polymers

Leilei Xiao[1,2], Casey Ching[3], Yuhan Ling[3], Mohammadreza Nasiri[4], Max J. Klemes[1], Theresa M. Reineke[4]*, Damian E. Helbling[3]*, William R. Dichtel[1]*

[1] *Department of Chemistry, Northwestern University, Evanston, IL 60208 USA*
[2] *Department of Chemistry and Chemical Biology, Cornell University, Ithaca, NY 14853 USA*
[3] *School of Civil and Environmental Engineering, Cornell University, Ithaca, NY 14853 USA*
[4] *Department of Chemistry, University of Minnesota, Minneapolis, MN 55455 USA*

Abstract

Per- and poly fluorinated alkyl substances (PFASs), notably perfluorooctanoic acid (PFOA) and perfluorooctanesulfonic acid (PFOS), contaminate many ground and surface water resources and are environmentally persistent. Furthermore, there are many other PFASs in use and many are likewise persistent and found to contaminate fresh water resources. A polymer consisting of β-cyclodextrin (β-CD) crosslinked with decafluorobiphenyl (DFB-CDP) has shown promise for sequestering PFOA at environmentally relevant concentrations, though its efficacy to remove other PFASs from water has not yet been explored. Additionally, although the DFB-CDP was designed to sequester PFASs on the basis of favorable fluorous interactions, the rationale for its relatively high affinity for PFOA compared to other previously synthesized β-CD polymers remains unknown. In this study, we explored crosslinker chemistry as a potential determinant of PFAS affinity for β-CD polymers. We synthesized three DFB-CDP derivatives with varying degrees of phenolation in the crosslinker (to evaluate effects of polymer surface charge) along with two β-CD polymers crosslinked by two other chemically distinct strategies, epichlorohydrin and 2-isocyanatoethyl methacrylate. We measured the equilibrium removal of ten PFASs from water by each of the five polymers at environmentally relevant concentrations. We found that β-CD polymers crosslinked by perfluorinated aromatics with low degrees of phenolation are more favorable for PFASs adsorption. These findings provide insight into the mechanism of PFASs adsorption by β-CD-based polymers and will inspire modular designs of β-CD-based adsorbents to target other PFASs and micropollutants.

Introduction

The contamination of ground and surface water by per-and polyfluorinated alkyl substances (PFASs), notably perfluorooctanoic acid (PFOA) and perfluorooctanesulfonic acid (PFOS), has emerged as an environmental and health crisis throughout the world.[1-2] PFASs are used in the production of fluoropolymers,[3-4] aqueous film-forming foam (AFFF) formulations to suppress fires,[5-6] and many other industrial processes and consumer products.[4,7-8] Because of the widespread usage of PFOA and PFOS, their ecological persistence, and their noted occurrence in drinking water resources, several communities in the United States declared states of emergency for PFOA and PFOS in 2016. Furthermore, although these two contaminants have drawn significant regulatory and legal attention, there are many other PFASs in use.[9] Granular activated carbon (GAC) is presently used as an adsorbent-of-last-resort in affected communities, but its intermediate affinity for PFASs makes it expensive to achieve residual aqueous phase concentrations below the regulatory thresholds.[10] GAC is also fouled by natural organic matter (NOM),[11] and regeneration of PFAS-loaded GAC is energy-intensive.[12]

β-cyclodextrin (β-CD), a macrocycle composed of seven glucose units, forms host–guest complexes with a variety of PFASs.[13] For instance, the association constants of the 1:1 host-guest complex between β-CD and PFOA and PFOS are $(5.00 \pm 0.10) \cdot 10^5$ M^{-1} and $(6.96 \pm 0.79) \cdot 10^5$ M^{-1} respectively.[14] Despite these relatively high association constants, some previous β-cyclodextrin-based polymers remove PFOA poorly, including a β-CD polymer crosslinked by tetrafluoroterephthalonitrile (**TFN-CDP**) that rapidly removes many organic chemicals from water.[15-16] Recently we reported a β-cyclodextrin (β-CD)-based polymer network, referred to as **DFB-CDP**, that reduces PFOA concentrations from 1 μg L^{-1} to <10 ng L^{-1}.[17] The adsorbent was not fouled by humic acids, which are major constituents of NOM, and was regenerated and reused multiple times by washing with MeOH. These characteristics make **DFB-CDP** a promising candidate for PFOA remediation. Although **DFB-CDP** was designed to stabilize β-CD-PFAS inclusion complexes through secondary noncovalent interactions with the crosslinkers, these interactions and the effects of crosslinker chemistry on PFASs uptake are not yet understood.

Recently we reported a side reaction during the polymerization of **TFN-CDP** in which a fluorine of TFN could be substituted by a hydroxyl group and the resulting phenolated TFN could be incorporated into the polymer network. More heavily phenolated polymers showed increased capacity to bind Pb^{2+} ions and increased binding affinity for 83 micropollutants,[18] yet all of the phenolated TFN-linked polymers had low affinity to anionic PFASs suggesting that phenolation may not be desired in β-CD polymers designed for PFAS uptake. Here we explore the role of crosslinker chemistry in modulating the removal of PFOA, PFOS and eight other PFASs. Within the **DFB-CDP** family, we explore the role of phenolation on the kinetics and thermodynamics of PFAS uptake. Noting the large difference in affinity between the **DFB-CDP** and β-CD polymers crosslinked by TFN, we also explored β-CD polymers crosslinked by two other chemically distinct strategies: epichlorohydrin, (**EPI-CDP**), a commonly studied CD-based adsorbent, and a urethane-containing methacrylate β-CD network (**IEM-CDP**) (**Scheme 1**). This broad comparison demonstrates that the nature of the crosslinkers plays an important role in PFAS uptake, and the superior PFASs uptake shown by the **DFB-CDP** establishes design criteria for further improving PFASs uptake.

Scheme 1

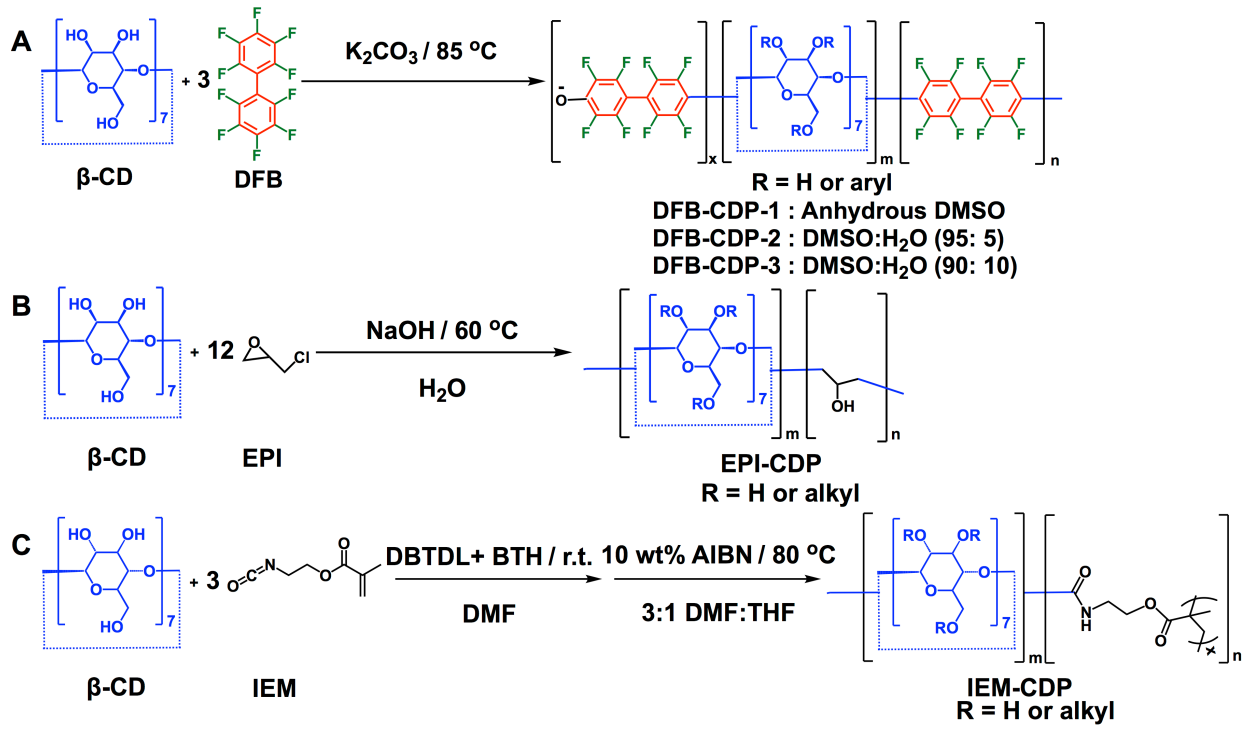

Results and Discussion

Model Studies. Because **DFB-CDP** is insoluble, it is difficult to determine the regiochemistry of the ether linkages and side reactions formed during polymerization. Model reactions of DFB with *n*-butanol in anhydrous DMSO imitate the reactions of hydroxyls of β-CD with DFB (**Scheme 2**). The dominant product observed by ^{19}F NMR was the 4,4′-dibutyl ether **1a** (83.5%), and minor products include the mono-phenolated **1b** (4.9%) and mono-phenolated, mono-butyl ether **2b** (7.7%) (**Scheme 2**). The presence of **2b** suggests the possibility of phenolated DFB being incorporated into the β-CD polymer network.

To control the side reactions and tune the concentrations of phenolated DFB incorporated into the polymer, we added 5% and 10% water to anhydrous DMSO to favor increased phenolation (**Scheme 2**). The formation of dibutyl ether **1a** is inhibited in reactions **2** and **3** compared with that in reaction **1**, with only 60.8% and 48.3% of **1a** being detected after 48 hours (**Scheme 2**). The phenolated product **2b** was formed in increased yield, with 21.4% of **2b** in reaction **2** and 35.8% in reaction **3** (**Scheme 2**). These experiments demonstrate that phenolation occurs readily in the presence of water. This model study suggests that polymerizations conducted with increased water content will provide **DFB-CDP** samples with higher amounts of phenolation.

Scheme 2

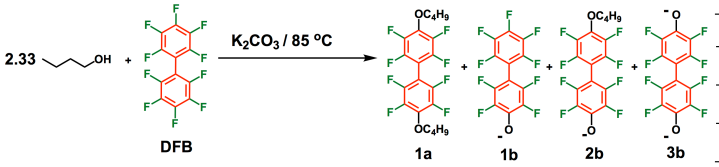

Reaction	Solvent	1a	1b	2b	3b
1	Anhydrous DMSO	83.5	4.9	7.7	0
2	DMSO: H_2O (95: 5)	60.8	13.2	21.4	2.5
3	DMSO:H_2O (90:10)	48.3	10.2	35.8	6.4

Polymer Synthesis and Characterization of DFB-CDPs. To tune the degree of phenolated DFB incorporated into **DFB-CDP** polymers while keeping the structure morphology of **DFB-CDPs** as similar as possible, we polymerized β-CD and DFB with the same molar feed ratio 1:3 in different solvents (DMSO: H_2O = 100: 0, 95:5, 90:10). After the monomers and K_2CO_3 were heated in solvents at 85°C, the suspensions gelled and were isolated in this form after 40-48 h (**Scheme 1**). Gels exhibited darker colors from polymer **DFB-CDP-1** to **DFB-CDP-3**, with the colors ranging from light yellow to light brown. Elemental analysis results of C, H, and F suggested that **DFB-CDPs** have similar crosslinking densities, with β-CD: DFB incorporation ratios ranging from 1:2.5 to 1:2.9 (**Table 1**). Meanwhile, **DFB-CDPs** had different concentrations of phenolated DFB incorporated into the polymers. The phenolate concentration in the polymers was determined by deprotonating the phenols using Li_2CO_3 and determining the amount of bound Li^+ using inductively coupled plasma optical emission spectroscopy (ICP-OES).[18] **DFB-CDP-1** has the lowest phenolate concentration at 0.063 ± 0.008 mmol g^{-1}, which indicates that 4.8 ± 0.6% of DFB incorporated into the polymer is phenolated. Meanwhile, **DFB-CDP-2** and **DFB-CDP-3** have similar and much higher phenolate concentrations incorporated into the polymers, with the values being 0.22 ± 0.011 mmol g^{-1} (16.1 ± 0.8% phenolated DFB) for **DFB-CDP-2** and 0.25 ± 0.018 mmol g^{-1} (17.4 ± 1.3% phenolated DFB) for **DFB-CDP-3**. These results are consistent with the model studies (**Scheme 2**) and demonstrate a way to control the phenolate concentration in the **DFB-CDPs**.

Table 1

Sample	β-CD: Crosslinker Incorporation Ratio	[Li^+] Bound (mmol g^{-1})	[Phenolate] (mmol g^{-1})
DFB-CDP-1	1:2.5	0.063±0.008	0.063±0.008
DFB-CDP-2	1:2.6	0.22±0.011	0.22±0.011
DFB-CDP-3	1:2.9	0.25±0.018	0.25±0.018
EPI-CDP	1:8	0*	N/A
IEM-CDP	1:3.5	0.031±0.009	N/A

* Li^+ signals of EPI-CDP samples by ICP-OES are below quantification limit.

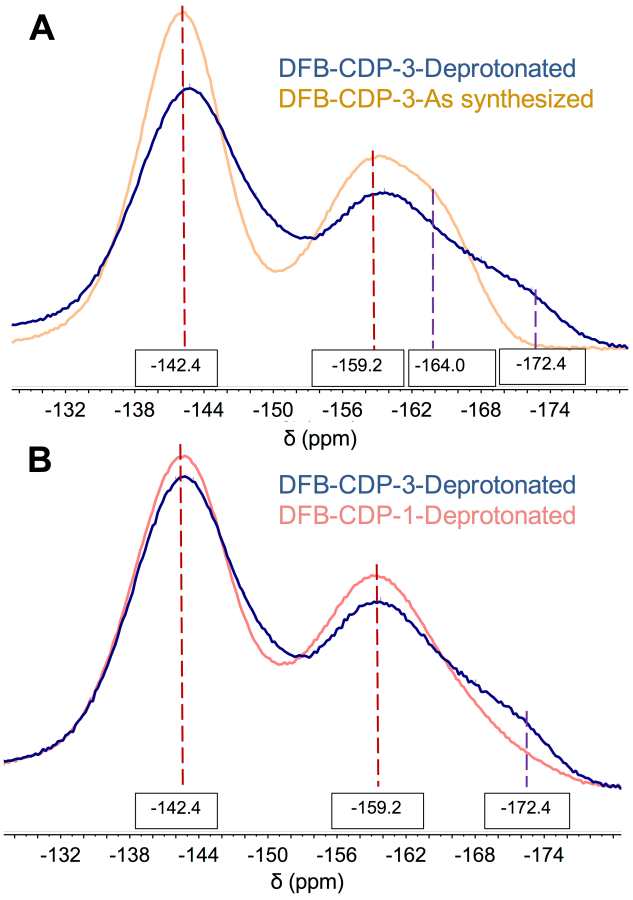

Figure 1. ^{19}F MAS NMR of DFB-CDPs at 600 MHz while spinning at 48 kHz. **A.** ^{19}F MAS NMR of as-synthesized and deprotonated DFB-CDP-3. Orange trace: As-synthesized DFB-CDP-3; Blue trace: DFB-CDP-3-Deprotonated; **B.** ^{19}F MAS NMR of deprotonated DFB-CDPs. Red trace: DFB-CDP-1-Deprotonated; Blue trace: DFB-CDP-3-Deprotonated.

The presence and relative concentrations of phenolates in the polymers were further confirmed by zeta potential measurements (**Table S2**) and solid-state ^{19}F NMR (**Figure S3**). The ^{19}F MAS NMR spectrum of as-synthesized **DFB-CDP-3** exhibited two broad peaks at -142.4 and -159.2

ppm (**Figure 1A**). These chemical shifts are similar to those found in the ^{19}F NMR spectrum of model compound **1a** obtained in solution (δ= -142.9 and -159.0 ppm). This observation indicates that the DFB-CDP polymers are linked mostly by 4,4'-disubstituted decafluorobiphenyl groups. The spectrum of as-synthesized **DFB-CDP-3** also exhibits a shoulder around -164.0 ppm, which corresponds to the fluorines adjacent to the phenol in the neutral form of **2b** (**2b'**, δ = -163.3 ppm, **Figure S1**). Upon treatment of **DFB-CDP-3** with K_2CO_3 to deprotonate the as-synthesized polymer, the chemical shifts of the shoulder shifted to -172.4 ppm, and a similar shift was observed in the solution spectrum of **2b** upon deprotonation (δ = -171.4 ppm, **Figure S1**). These observations suggest that the shoulder corresponds to fluorines on phenolated aryl rings that are incorporated into **DFB-CDP-3**. Notably, the shoulder at -172.4 ppm is much less prominent in the spectrum of the less-phenolated **DFB-CDP-1 (Figure 1B)**, which is consistent with the loadings determined by ICP-OES.

PFOA Adsorption in Nanopure Water by DFB-CDPs. The degree of phenolation incorporated into **DFB-CDPs** was inversely associated with their PFOA equilibrium removal percentage. The PFOA removal efficiency of each sample was characterized in a batch experiment using $[PFOA]_0$ of 1 μg L^{-1} in nanopure water, and [**DFB-CDP**] of 10 mg L^{-1}. Each adsorbent was sieved to between 20 μm and 45 μm to minimize differences in adsorption behavior that can be attributed to differences in particle sizes. Each of the **DFB-CDPs** adsorbs PFOA under these conditions and exhibits similar adsorption kinetics when comparing the rates of adsorption using Ho and McKay's pseudo-second-order adsorption model (**Figure 2**).[19] The values of k_{obs} from 0 to 6 h are 34.0, 30.4 and 39.3 g mg^{-1} h^{-1} for **DFB-CDP-1**, **DFB-CDP-2** and **DFB-CDP-3** respectively. **DFB-CDP-1** removed 86.6 ± 7.1% of PFOA at equilibrium, while **DFB-CDP-2** and **DFB-CDP-3** exhibited 68.2 ± 1.5% and 65.0±2.1% equilibrium removal of PFOA (**Table 2**). The average PFOA removal at equilibrium was inversely associated to the phenolation levels of DFB-CDPs 1-3. Therefore, through comparing three **DFB-CDPs** with similar crosslinking density and morphology, these experiments demonstrate that the thermodynamics of PFOA uptake by β-CD polymers are negatively influenced by the presence of phenolates.

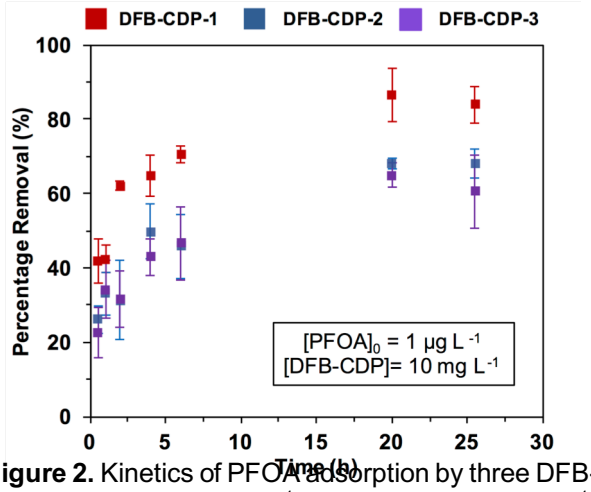

Figure 2. Kinetics of PFOA adsorption by three DFB-CDPs ($[PFOA]_0$ = 1 μg L^{-1}; [DFB-CDP] = 10 mg L^{-1}) in nanopure water. Error bars: Standard deviation of 3 experiments.

Table 2

Adsorbent	Equilibrium Removal (%)	k_{obs} (g mg^{-1} h^{-1})
DFB-CDP-1	86.6±7.1	34.0
DFB-CDP-2	68.2±1.5	30.4
DFB-CDP-3	65.0±2.1	39.3

Polymer Synthesis and Characterization of EPI-CDP and IEM-CDP. Two other β-CD-based polymers were prepared and evaluated to further understand how crosslinker chemistry influences PFASs adsorption. Epichlorohydrin-cyclodextrin polymer (**EPI-CDP, Scheme 1B**) was selected because it has been studied extensively as an alternative adsorbent and lacks hydrophobic crosslinkers.[20] Another β-CD polymer was prepared by modifying β-CD with 2-isocyanatoethyl

methacrylate (IEM), followed by radical polymerization of the methacrylate groups (**IEM-CDP**, **Scheme 1C**). IEM-CDP was designed as a more hydrophobic polymer that lacks perfluoroarene linkers. Both materials were formed as insoluble, water swellable solids with structural parameters given in the SI.

PFAS Adsorption Studies. The three **DFB-CDPs**, **EPI-CDP**, **IEM-CDP** were evaluated for their ability to remove a mixture of ten PFASs with different chain lengths and polar head groups. Six PFASs are perfluoroalkyl carboxylic acids (PFCAs) with n = 4, 6, 7, 8, 9, and 10 carbons, three are perfluoroalkyl sulfonates (PFSAs) with n = 4, 6, and 8 carbons, and the tenth PFAS is an ammonium perfluoroalkyl ether carboxylate associated with the Chemours GenX process.

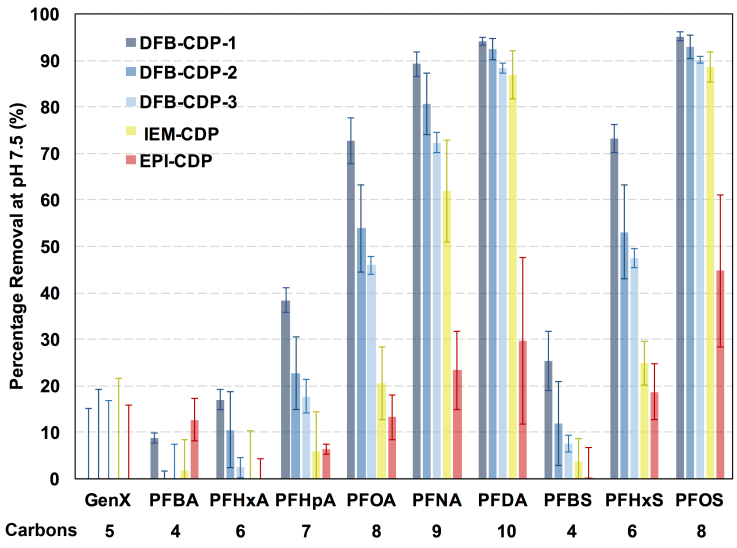

Figure 3. Equilibrium adsorption of ten PFASs by five β-CD-based polymers in 1 mM pH 7.5 phosphate buffer ($[PFAS]_0$ = 1 μg L^{-1}; [Adsorbent] = 10 mg L^{-1}). Error bars: Standard deviation of 3 experiments.

Batch experiments were performed to evaluate the equilibrium removal (contact time = 9 hours) of 1 μg L^{-1} of each PFAS in the presence of each of the five CD-based adsorbents (10 mg L^{-1}) in a 1 mM phosphate buffer solution at pH 7.5 (**Figure 3**). **DFB-CDP-1** performed the best and exhibited more than 70% removal of PFOA, PFNA, PFDA, PFHxS and PFOS, along with modest removal of some shorter-chain PFASs, with 5–40% equilibrium removal noted for PFBA, PFHxA, PFHpA, and PFBS. The trend of higher affinity for longer-chain PFASs was observed for all five β-CD-based polymers, indicating that the hydrophobic interaction between β-CD-based polymers and PFASs is affecting β-CD-based polymers' affinity for PFASs. Likewise, all five β-CD-based polymers exhibited better removal of perfluorosulfonic acids (PFSA) than perfluorocarboxylic acids (PFCA) with the same carbon number (except for PFBA and PFBS removal by **EPI-CDP**), which is consistent with the adsorption affinity of GAC, anion exchange resins, and other adsorbents for PFASs.[21-22] Notably, none of the five β-CD-based polymers exhibited significant removal of GenX. Weiss-Errico and coworkers found that β-CD binds GenX two orders of magnitude more weakly than PFOA because of GenX's branched structure ($K_a = (7.45 \pm 4.27) \cdot 10^2$ M^{-1}), which is consistent with the poor removal of GenX by all five β-CD-based polymers observed here. Furthermore, the observation of poor GenX uptake suggests that β-CD is involved during the adsorption of the other PFASs.[13]

Among the three **DFB-CDP** polymers, **DFB-CDP-2** and **DFB-CDP-3** exhibited similar and lower equilibrium removal of several PFAS than **DFB-CDP-1**, including PFHpA, PFOA, PFNA, PFBS and PFHxS. This observation is consistent with the 1 μg L^{-1} PFOA adsorption results in nanopure water (**Figure 2**) and can be explained by more phenolated DFB incorporated into the polymer network of **DFB-CDP-2** and **DFB-CDP-3** than **DFB-CDP-1**. The other two β-CD-based polymers linked with epichlorohydrin (**EPI-CDP**) and 2-isocyanatoethyl methacrylate (**IEM-**

CDP) exhibited significantly lower removal for 8 out of 10 PFASs than the three **DFB-CDPs**, in which **EPI-CDP** had the poorest performance and removed no more than 50% of any PFAS at equilibrium. These results are informative considering that both **EPI-CDP** and **IEM-CDP** exhibited less negative zeta potential values at pH 7.5 than **DFB-CDPs**, with **EPI-CDP** being close to neutral, -1.29 ± 0.55 mV, and **IEM-CDP** being -9.16 ± 0.43 mV. This suggests that surface charge may be one important factor, but not the only factor that determines a β-CD-based polymer's affinity for anionic PFASs.

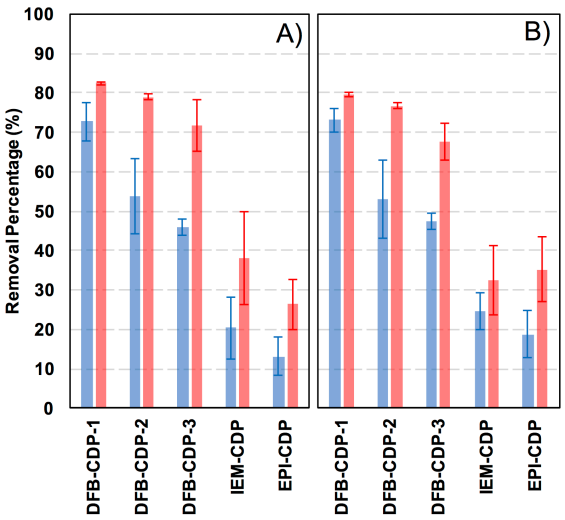

Figure 4. Comparison of equilibrium removal % for (A) PFOA and (B) PFHxS by five β-CD-based polymers at pH 7.5 (blue) and 5.5 (red). ($[PFAS]_0$ = 1 μg L^{-1}; [Adsorbent] = 10 mg L^{-1}; Matrix: 1 mM phosphate buffer). Error bars: Standard deviation of 3 experiments.

To further evaluate the role of surface charge on PFAS uptake, we repeated the PFAS experiments in a 1 mM phosphate buffer solution at pH 5.5. The surface charge of four of the five polymers (all except for EPI-CDP) became less negative at pH 5.5. All β-CD-based polymers exhibited improved removal for the majority of the PFASs at pH 5.5 than at pH 7.5 (**Figure S7**). **Figure 4** shows the comparison of equilibrium removal percentage of PFOA and PFHxS at pH 7.5 and pH 5.5 among the five polymers. Each polymer exhibited a broad-spectrum increase of PFAS removal when the pH was lowered from 7.5 to 5.5. The performance gain was largest for polymers that exhibited relatively poor removal of a particular PFAS at pH 7.5. For example, among the three **DFB-CDPs**, the increase in removal of PFOA at pH 5.5 was greater for **DFB-CDP-2** and **DFB-CDP-3**. Similarly, the increase in removal of PFHxS at pH 5.5 was greater for **DFB-CDP-2** and **DFB-CDP-3**. This further demonstrates the role that polymer surface charge plays in the removal of PFASs among structurally similar β-cyclodextrin polymers. The performance of the **EPI-CDP** polymer also increased at pH 5.5 despite more subtle changes in the surface charge. For example, the surface charge of **EPI-CDP** is -1.29 ± 0.55 mV and -0.87 ± 0.23 mV at pH 7.5 and 5.5, respectively. These results suggest that the enhanced removal of PFASs at lower pH is not only due to the protonation of β-CD-based polymers' functional groups, but other factors such as the chemical nature of the PFAS. Moreover, despite the fact that **EPI-CDP** exhibited better removal of PFAS at pH 5.5, the performance of **EPI-CDP** remains modest, with removal of all PFAS except PFOS remaining less than 50% (**Figure S7**). This further demonstrates that other properties of β-CD-based polymers are affecting their affinity to PFAS besides surface charge. Taken together, our data suggests that an optimized microenvironment around β-CD is essential for maximum affinity for PFASs, which is the combination of crosslinker chemistry, crosslinking density,[17] and surface charge.

Conclusions

Three decafluorobiphenyl β-CD crosslinked polymers with similar crosslinking density and different amounts of phenolated decafluorobiphenyl incorporated into the polymer network were synthesized. Both zeta potential measurement and ^{19}F MAS NMR of the three polymers are consistent with the presence and concentrations of phenolated decafluorobiphenyl in the polymer network. **DFB-CDP-1**, the polymer with the lowest phenolate concentration, exhibited the highest

affinity for PFOA in nanopure water, and for 10 PFASs in buffered solutions as well. These findings suggest that negative charges around β-CD hinder the capture of negatively charged PFASs. Two other β-CD-based polymers with different crosslinkers, epichlorohydrin and 2-isocyanatoethyl methacrylate, were synthesized and showed inferior affinity compared to **DFB-CDPs** for 8 out of 10 PFASs. This finding indicates that other properties of β-CD-based polymers besides zeta potential will affect their affinity for PFASs, such as the chemical nature of the crosslinker and the crosslinking density. Finally, this study demonstrates that the affinity of β-CD-based polymer adsorbents to certain micropollutants can be tuned through the judicious modification of their composition.

ASSOCIATED CONTENT

Supporting Information. The Supporting Information is available from the *ChemRxiv* preprint server.

AUTHOR INFORMATION

Corresponding Authors

W. R. Dichtel; wdichtel@northwestern.edu
D. E. Helbling; damian.helbling@cornell.edu
T. M. Reineke: treineke@umn.edu

Notes

The authors declare the following competing financial interest(s): W.R.D. And D.E.H. own equity and/or stock options in CycloPure Inc., which is commercializing materials related to those reported in this work.

Acknowledgements

This research was supported by NSF through the Center for Sustainable Polymers (CHE-1413862) and by the Strategic Environmental Research and Development Program (ER18-1026). This work made use of the IMSERC at Northwestern University, which has received support from the NSF (CHE-1048773); Soft and Hybrid Nanotechnology Experimental (SHyNE) Resource (NSF ECCS-1542205); the State of Illinois and International Institute for Nanotechnology (IIN); the EPIC facility of Northwestern University's NUANCE Center, which has received support from the Soft and Hybrid Nanotechnology Experimental (SHyNE) Resource (NSF ECCS-1542205); the MRSEC program (NSF DMR-1720139) at the Materials Research Center; the International Institute for Nanotechnology (IIN); the Keck Foundation; and the State of Illinois, through the IIN. We thank Dr. Riqiang Fu for conducting ^{19}F MAS NMR experiments at the National High Magnetic Field Lab (NHMFL) supported by the NSF Cooperative agreement No. DMR-1644779 and the State of Florida.

References

(1). Clara, M.; Gans, O.; Weiss, S.; Sanz-Escribano, D.; Scharf, S.; Scheffknecht, C., *Water Res*. **2009,** *43*, 4760-4768.
(2). Rumsby, P. C.; McLaughlin, C. L.; Hall, T., *Philos. Trans. Royal Soc. A* **2009,** *367*, 4119-4136.

(3). Herzke, D.; Olsson, E.; Posner, S., *Chemosphere* **2012,** *88*, 980-987.
(4). Buck, R. C.; Franklin, J.; Berger, U.; Conder, J. M.; Cousins, I. T.; de Voogt, P.; Jensen, A. A.; Kannan, K.; Mabury, S. A.; van Leeuwen, S. P., *Integr Environ Assess Manag*. **2011,** *7*, 513-541.
(5). Barzen-Hanson, K. A.; Field, J. A., *Environ. Sci. Technol. Lett*. **2015,** *2*, 95-99.
(6). Place, B. J.; Field, J. A., *Environ. Sci. Technol*. **2012,** *46*, 7120-7127.
(7). Trier, X.; Granby, K.; Christensen, J. H., *Environ Sci Pollut Res Int*. **2011,** *18*, 1108-1120.
(8). Kotthoff, M.; Müller, J.; Jürling, H.; Schlummer, M.; Fiedler, D., *Environ Sci Pollut Res Int*. **2015,** *22*, 14546-14559.
(9). Xiao, X.; Ulrich, B. A.; Chen, B.; Higgins, C. P., *Environ. Sci. Technol*. **2017,** *51*, 6342-6351.
(10). Yu, Q.; Zhang, R.; Deng, S.; Huang, J.; Yu, G., *Water Res*. **2009,** *43*, 1150-1158.
(11). Yu, J.; Lv, L.; Lan, P.; Zhang, S.; Pan, B.; Zhang, W., *J. Hazard. Mater*. **2012,** *225-226*, 99-106.
(12). Watanabe, N.; Takata, M.; Takemine, S.; Yamamoto, K., *Environ Sci Pollut Res Int*. **2018,** *25*, 7200-7205.
(13). Weiss-Errico, M. J.; Ghiviriga, I.; O'Shea, K. E., *J. Phys. Chem. B* **2017,** *121*, 8359-8366.
(14). Weiss-Errico, M. J.; O'Shea, K. E., *J. Hazard. Mater*. **2017,** *329*, 57-65.
(15). Alsbaiee, A.; Smith, B. J.; Xiao, L.; Ling, Y.; Helbling, D. E.; Dichtel, W. R., *Nature* **2016,** *529*, 190-194.
(16). Ling, Y.; Klemes, M. J.; Xiao, L.; Alsbaiee, A.; Dichtel, W. R.; Helbling, D. E., *Environ. Sci. Technol*. **2017,** *51*, 7590-7598.
(17). Xiao, L.; Ling, Y.; Alsbaiee, A.; Li, C.; Helbling, D. E.; Dichtel, W. R., *J. Am. Chem. Soc*. **2017,** *139*, 7689-7692.
(18). Klemes, M. J.; Ling, Y.; Chiapasco, M.; Alsbaiee, A.; Helbling, D. E.; Dichtel, W. R., *Chem. Sci*. **2018,** *9,* 8883-8889.
(19). Ho, Y. S.; McKay, G., *Process Biochem*. **1999,** *34*, 451-465.
(20). Morin-Crini, N.; Crini, G., *Prog. Polym. Sci*. **2013,** *38*, 344-368.
(21). McCleaf, P.; Englund, S.; Östlund, A.; Lindegren, K.; Wiberg, K.; Ahrens, L., *Water Res*. **2017,** *120*, 77-87.
(22). Ateia, M.; Attia, M. F.; Maroli, A.; Tharayil, N.; Alexis, F.; Whitehead, D. C.; Karanfil, T., *Environ. Sci. Technol. Lett*. **2018,** *5,* 764–769.